K^+-aggravated myotonia: destabilization of the inactivated state of the human muscle Na^+ channel by the V1589M mutation

N. Mitrović*, A. L. George Jr†, R. Heine*, S. Wagner*, U. Pika*, U. Hartlaub*, M. Zhou†, H. Lerche*, Ch. Fahlke‡ and F. Lehmann-Horn*§

*Department of Applied Physiology, University of Ulm, D-89069 Germany, †Departments of Medicine and Pharmacology, Vanderbilt University Medical Center, Nashville, TN, USA and ‡Department of General Physiology, University of Ulm, D-89069 Germany

1. Wild type (WT) and V1589M channels were expressed in human embryonic kidney (HEK293) cells for the study of the pathophysiology of the V1589M muscle Na^+ channel mutation leading to K^+-aggravated myotonia.

2. In comparison to WT, whole-cell recordings with V1589M channels showed an increased Na^+ steady-state to peak current ratio (I_{ss}/I_{peak}) (3·15 ± 0·70 *vs.* 0·87 ± 0·10%, at −15 mV) and a significantly faster recovery from inactivation. The recovery time constants, τ_{r1} and τ_{r2}, were decreased from 1·28 ± 0·12 to 0·92 ± 0·08 ms and from 4·74 ± 0·94 to 2·66 ± 0·51 ms for the WT and mutant channels, respectively.

3. Single-channel recordings with mutant channels showed higher probability of short isolated late openings (0·40 ± 0·09 *vs.* 0·06 ± 0·02, at −30 mV) and bursts of late openings (0·011 ± 0·003 *vs.* 0·003 ± 0·001, at −30 mV) compared to WT.

4. These results suggest that the mutation increases the probabilities for channel transitions from the inactivated to the closed and the opened states.

5. Increased extracellular concentrations of K^+ had no effects on either V1589M or WT currents in HEK293 cells. The aggravation of myotonia seen in patients during increased serum K^+ may arise from the associated membrane depolarization which favours the occurence of late openings in the mutant channel.

Na^+ channel disease is the generic name for the syndromes caused by various mutations in the gene encoding the adult human muscle Na^+ channel (SCN4A). According to this definition, muscle Na^+ channel disease encompasses paramyotonia congenita (PC), hyperkalaemic periodic paralysis (HyperPP) and K^+-aggravated myotonia (PAM) (Rüdel, Ricker & Lehmann-Horn, 1993). PAM is characterized by episodes of muscle stiffness that are aggravated by the intake of K^+. In contrast to PC and HyperPP, muscle weakness is not a clinical symptom of PAM (Heine, Pika & Lehmann-Horn, 1993; Lerche *et al.* 1993).

Electrophysiological studies on muscle specimens excised from patients with various muscle Na^+ channel defects, or on myotubes cultured from such specimens, showed altered Na^+ channel inactivation (Lehmann-Horn, Küther, Ricker, Grafe, Ballanyi & Rüdel, 1987; Cannon, Brown & Corey, 1991; Lehmann-Horn, Iaizzo, Hatt & Franke, 1991; Lerche *et al.* 1993). As the yield of data and the reproducibility of results (and thus the information on the disease-causing character of a mutation) are higher when studies of the functional properties of SCN4A mutations are performed with transfected cells rather than native tissue, some human Na^+ channel mutations (T704M, M1592V, R1448H/C) have already been introduced in a rat or human Na^+ channel cDNA and expressed in cell lines (Cummins *et al.* 1993; Cannon & Strittmatter, 1993; Chahine *et al.* 1994). With each of these mutations the Na^+ channel inactivation was abnormal (Cannon & Strittmatter, 1993; Chahine *et al.* 1994).

V1589M is one of several Na^+ channel mutations causing PAM (Heine *et al.* 1993). Amino acid 1589 is located in the sixth transmembrane segment of the fourth Na^+ channel repeat, next to the helical position of the inverse substitution, M1592V, known to cause HyperPP associated

§To whom all correspondence should be addressed.

with myotonia (Rojas, Wang, Schwartz, Hoffman, Powell & Brown, 1991). In the present study we expressed transiently and permanently wild type (WT) and V1589M mutant human muscle Na^+ channels in the human embryonic kidney cell line HEK293 and describe their kinetics.

METHODS

Mutagenesis

Site-directed mutagenesis was performed with a 1588 bp *Hind*III–*Sac*I fragment of WT hSkM1 (nucleotides 4051–5639; George, Komisarof, Kallen & Barchi, 1992), which was subcloned into the plasmid pSELECT of the pSELECT mutagenesis system (Promega Corporation, Madison, WI, USA) and a mutagenic oligonucleotide (V1589M: 5′-ACA-TGTTGACCATGATGAGGAAGGA-3′). Full-length hSkM1–V1589M mutants were reassembled in the pRc/CMV plasmid (Invitrogen, San Diego, CA, USA) using a 1023 bp *Cla*I–*Sac*I fragment from the pSELECT construct containing the mutant sequence and other regions from the WT hSkM1. Plasmid DNA for mammalian transfection was prepared by adsorption to macroporous silica gel anion exchange columns (Qiagen, Chatsworth, CA, USA).

Transfection

To obtain cells expressing WT and V1589M Na^+ channels HEK293 cells (ATCC CRL 1573) were transfected by the calcium phosphate precipitation method (Graham & van der Eb, 1973) using the plasmids pRc/CMV–hSkM1 and pRc/CMV–V1589M, respectively. Transient expression was detected electrophysiologically 48–72 h after transfection. Oligoclonal cell lines were obtained by selection for resistance to the aminoglycoside antibiotic Geneticin (G418; Boehringer Mannheim, Germany). Twenty hours after transfection cells were incubated in medium supplemented with G418 (800 $\mu g\ ml^{-1}$). After 10–28 days cells were pooled and used in electrophysiological experiments.

To reproduce the mutant phenotype, plasmids from two different cloning procedures were transfected.

Electrophysiology

Standard whole-cell recording (Hamill, Marty, Neher, Sakmann & Sigworth, 1981) was performed at room temperature (~22 °C). The voltage error due to series resistance was < 5 mV. Leakage and capacitive currents were automatically subtracted by means of a prepulse protocol (−P/4) in all whole-cell recordings. Currents were filtered with an internal 3 kHz filter of the amplifier and digitized at a 20 kHz sampling rate using pCLAMP (Axon Instruments, Foster City, CA, USA). Data were analysed with pCLAMP and home-made software. The pipette solution contained (mM): 130 CsCl, 2 $MgCl_2$, 5 EGTA and 10 Hepes (pH 7·4). The bath solution contained (mM): 140 NaCl, 4 KCl, 2 $CaCl_2$, 1 $MgCl_2$, 4 dextrose and 5 Hepes (pH 7·4).

Single-channel currents were recorded from cell-attached patches. The bathing solution contained (mM): 130 CsCl, 2 $MgCl_2$, 5 EGTA, 10 Hepes (pH 7·4); the pipette solution contained (mM): 140 NaCl, 4 KCl, 2 $CaCl_2$, 1 $MgCl_2$, 4 dextrose, 5 Hepes (pH 7·4). The leakage and capacity transients were eliminated by subtracting averaged and scaled records without channel activity. The number of channels present in the patch was estimated by inspecting traces and counting the maximum number of the channels that open simultaneously (Aldrich, Corey & Stevens, 1983).

For statistic evaluation a 5% α-level was chosen and Student's t test applied. All data are shown as means ± S.E.M.

RESULTS AND DISCUSSION

Transfection of HEK293 cells

Permanent expression was achieved by selecting the cells for resistance to the aminoglycoside antibiotic G418. Na^+ currents were observed 48–72 h after the usual transient transfection and 10–28 days after the permanent transfection. The electrophysiological measurements were mainly performed in the G418-resistant cells since the expression rate was higher (80%) than in the transiently transfected cells (10%). The channel parameters analysed were not different for the two types of transfection.

One of the possible differences between native muscle Na^+ channels and expressed channels could be the absence of the β-subunit in the latter. This co-factor has been shown to be important for fast inactivation in the oocyte expression system (Isom *et al.* 1991). The mRNA encoding the β-subunit is present in the transfected HEK cells (authors' unpublished observations) but the expression rate of this endogenous β-subunit is not known.

Steady-state sodium currents seen in whole-cell recordings

Peak Na^+ current amplitudes (I_{peak}) ranged from 0·6 to 20 nA for WT channels (mean 6·07 ± 0·79 nA, mean cell capacitance 36 ± 5 pF, $n = 21$) and from 0·5 to 22 nA for V1589M channels (mean 5·98 ± 0·89 nA, mean cell capacitance 38 ± 6 pF, $n = 23$). HEK cells also express endogenous Na^+ channels that conduct current with amplitudes ranging from 50 to 350 pA (mean 112 ± 12 pA, mean cell capacitance 34 ± 3 pF, $n = 20$). To minimize a possible contribution of endogenous Na^+ channels, but also to avoid large series resistance errors, we only analysed currents with I_{peak} ranging between 2 and 5 nA.

Figure 1*A* shows Na^+ currents elicited by various depolarization steps from a common prepulse potential of −120 mV (holding potential −85 mV). The I_{peak}–V relationships for WT and mutant Na^+ channels were almost identical (Fig. 1*B*). The non-inactivating, steady-state current, I_{ss}, quantified 35 ms after the onset of the depolarizing pulse when the current had reached a plateau, was normalized to the maximum steady-state current recorded in the entire test range. With respect to the I_{peak} curve, the I_{ss}–V relationship was shifted by 15 mV in the hyperpolarizing direction (Fig. 1*B*). Consequently, I_{ss} was normalized to I_{peak} and, as shown in Fig. 2*A*, was considerably larger with mutant than with WT channels. The difference was more pronounced the smaller the depolarization. I_{ss} was never seen in non-transfected or mock-transfected cells. Since I_{ss} resembles leak currents, tetrodotoxin (TTX) was applied to five cells having mutant

channels and to two cells having WT channels. I_{ss} (and I_{peak}) was blocked > 90% by 1 μM TTX. Therefore, we concluded that I_{ss} was conducted by WT and mutant channels.

With mutant channels, I_{ss} was 3–4% of I_{peak}. Assuming that, in contrast to a value of 100% in HEK cells, in a patient's muscle 50% of the channels are of the mutant type (dominant mode of inheritance), the corresponding *in vivo* I_{ss} would amount to 2% (1·5–2% mutant plus 0·4% WT). An I_{ss}/I_{peak} ratio of 5% (rat model; Cannon & Corey, 1993) or 2% (computer model; Cannon, Brown & Corey, 1993) is sufficient to produce myotonia. According to the computer model, the late current observed in our experiments would be on the 'myotonic border'.

Inactivation and activation of currents conducted by the mutant channels

To test for differences between WT and mutant inactivation, the decay of the current amplitudes, I, was approximated by the sum of two exponentials according to:

$$I/I_{peak} = g_1 \exp(-t/\tau_{h1}) + g_2 \exp(-t/\tau_{h2}) + I_{ss}/I_{peak},$$

where t is the time elapsed from the beginning of the depolarizing step, τ_{h1} and τ_{h2} are the time constants of inactivation, and g_1 and g_2 are the relative amplitudes of the two exponentials. Both the fast (τ_{h1}) and the slow (τ_{h2}) time constants were voltage dependent and did not differ with WT and mutant channels (Fig. 2*B*). The amplitude factor g_2 of the slow component was significantly increased in mutant channels as shown in Fig. 2*C*.

For the examination of the voltage dependence of steady-state inactivation, a variable prepotential (from −150 to 0 mV) preceded constant test pulses to 0 mV (−85 mV holding potential). The steady-state inactivation curves (Fig. 2*D*) were fitted with the standard Boltzmann distribution ($I/I_{max} = (1 + \exp[(V - V_{0.5})/k])^{-1}$). $V_{0.5}$ values were −52·7 ± 2·8 and −47·3 ± 1·2 mV, and the reciprocal slopes, k, were 8·2 ± 0·3 and 8·8 ± 0·2 mV, for WT and mutant channels, respectively. Thus, the mutant inactivation curve was shifted by 5–6 mV in the depolarizing direction.

Recovery from inactivation

For the determination of this parameter the cells were depolarized for 12 ms to 0 mV (to inactivate Na^+ channels), then repolarized to the recovery potential of −100 mV for increasing durations prior to a test pulse to 0 mV. Recovery was faster for V1589M than for WT channels (Fig. 3). The time course of the recovery was best fitted by:

$$I/I_{max} = (a - b)\exp(-t/\tau_{r1}) + (b - a)\exp(-t/\tau_{r2}).$$

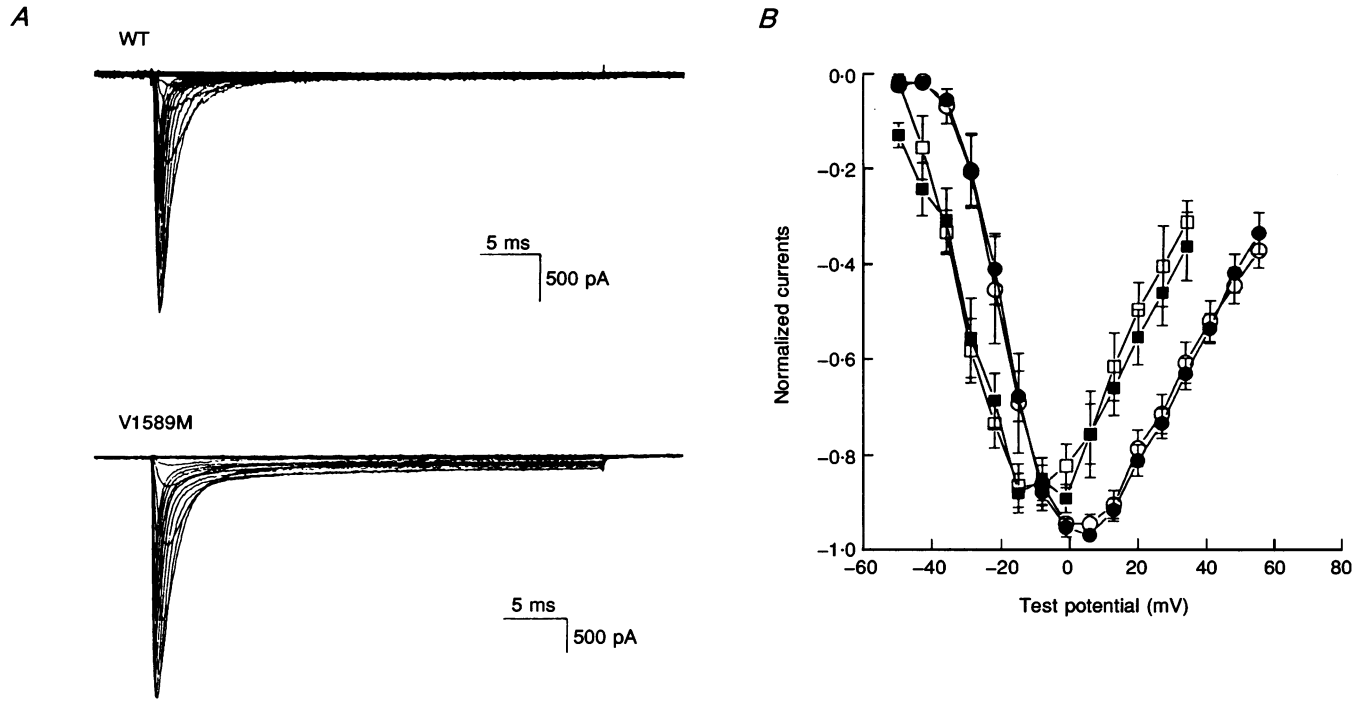

Figure 1. Effect of V1589M mutation on whole-cell Na^+ currents
A, representative current recordings from HEK293 cells transfected with either WT or V1589M. After a 15 ms prepulse to −120 mV (holding potential −85 mV) currents were elicited by test potentials from −50 to +55 mV in 7 mV steps. *B*, normalized current–voltage relationships for both peak (circles, $I_{peak}/(I_{peak})_{max}$) and steady-state currents (squares, $I_{ss}/(I_{ss})_{max}$) in WT (open symbols) and mutant channels (filled symbols). Mean values ± S.E.M. (n = 8–10).

The time constants, τ_{r1} and τ_{r2}, were decreased from 1·28 ± 0·12 to 0·92 ± 0·08 ms and from 4·74 ± 0·94 to 2·66 ± 0·51 ms for the WT and mutant channels, respectively. The time course of the recovery from inactivation at −80 mV was best fitted with a single exponential and was also faster in V1589M ($\tau_r = 2{\cdot}42 \pm 0{\cdot}17$, $n = 4$) than in WT channels ($\tau_r = 4{\cdot}47 \pm 0{\cdot}34$, $n = 6$).

The faster recovery from inactivation in the mutant channels is another factor that might contribute to the tendency of a muscle fibre to produce myotonic runs. The refractory period following an action potential is abbreviated and the effect of I_{ss} on the generation of action potentials could be enhanced.

Effect of extracellular K^+ ($[K^+]_o$)

As a characteristic clinical symptom of the Na^+ channel disease PAM, patients experience serious aggravation of myotonia when their serum K^+ is increased. We therefore examined the effect of 9 mM $[K^+]_o$ on the Na^+ currents of cells expressing mutant ($n = 8$) and WT ($n = 12$) Na^+ channels. In neither case did we find a statistically significant increase of I_{ss}.

In intact, not voltage-clamped muscle fibres, excised from patients having a Na^+ channel mutation, high $[K^+]_o$ did produce a substantial increase of Na^+ influx (Lehmann-Horn *et al.* 1987). Our result showing an unchanged I_{ss} in high $[K^+]_o$ may be explained in the following way. *In vivo*, the elevated $[K^+]_o$ produces a slight membrane depolarization and this causes repetitive activity, as demonstrated in such excised muscles (Lehmann-Horn *et al.* 1987). In the V1589M mutant, depolarization also favours the occurrence of late Na^+ channel activity, but the depolarizing effect of K^+ can of course not be detected under voltage-clamp conditions.

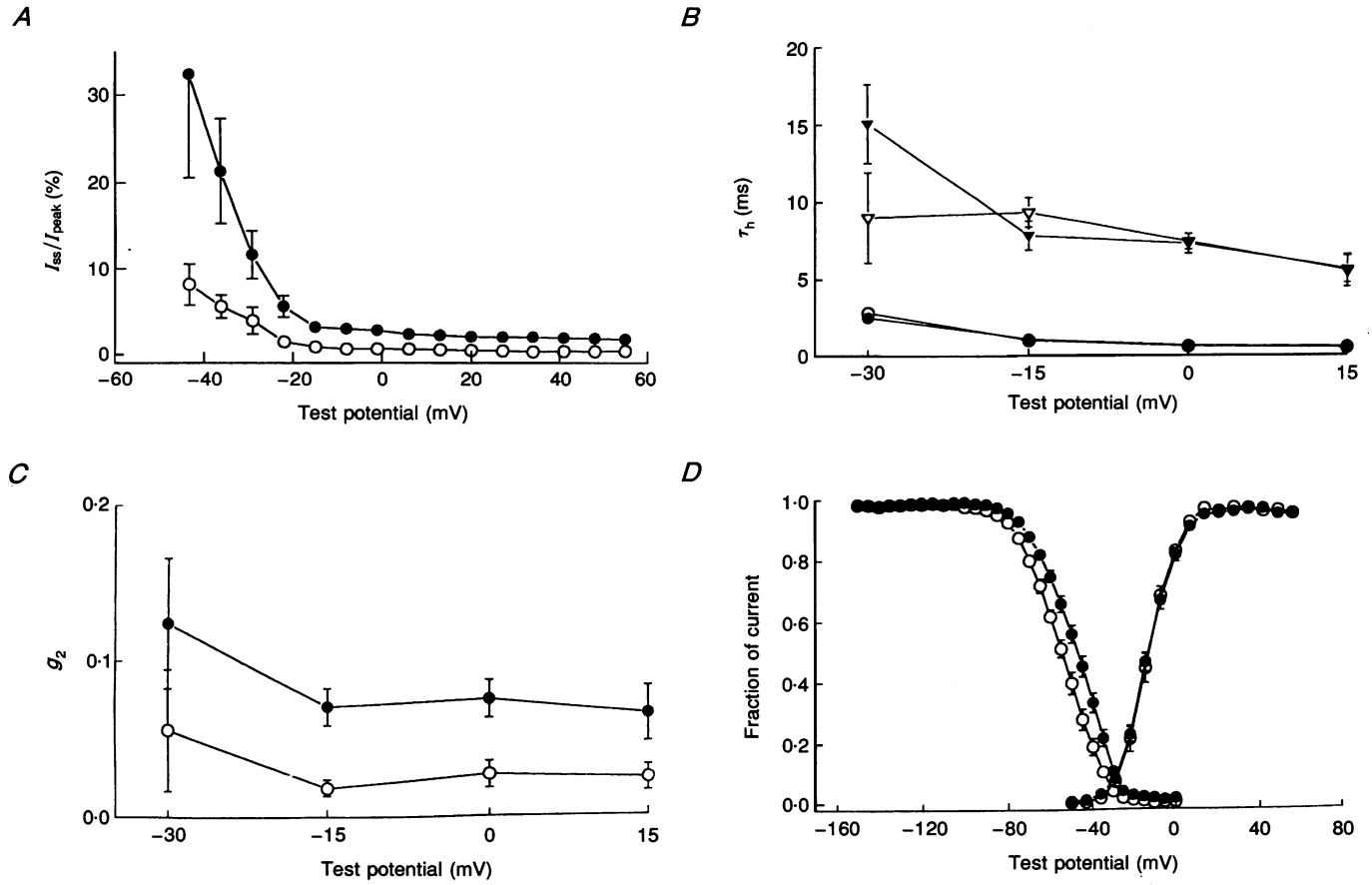

Figure 2. Na^+ WT and V1589M channel inactivation parameters
A, non-inactivating, steady-state current (I_{ss}) normalized to peak current (I_{peak}). Cells held at −85 mV and depolarized to test potentials from −43 to +55 in 7 mV steps after a 15 ms prepulse to −120 mV. I_{ss} analysed 35 ms after onset of depolarization. ○, WT; ●, V1589M; $n = 8$. *B*, time constants of inactivation (τ_h) for currents elicited by step depolarizations from the holding potential of −100 mV as a function of membrane potential. The decay of the current was best fitted with two inactivation time constants, fast (τ_{h1}, circles) and slow (τ_{h2}, triangles) in both types of channels. *C*, amplitude factor g_2 of the slow phase of Na^+ channel inactivation plotted against test potential. Data from 8–10 cells expressing either WT (open symbols) or mutant channels (filled symbols). *D*, plot of the WT ($n = 8$–10) and V1589M ($n = 8$–10) steady-state inactivation and activation of the Na^+ current. Inactivation induced by 15 ms prepulse varying from −150 to 0 mV before test pulses to 0 mV (holding potential −85 mV).

Single-channel recordings

Na^+ currents were elicited in thirty cell-attached patches of twenty transfected HEK293 cells by depolarizing voltage steps starting from a holding potential of −100 mV. Their amplitudes ranged from 0 to 200 pA. Figure 4 shows current traces from a patch containing three WT channels (*A*) and three mutant channels (*B*) after a jump to a test potential of −30 mV. Following the current peak, late channel openings occurred either as short single events or bursts, as shown in the fourth traces of Fig. 4*A* and *B*. According to these observations we defined three gating modes (Patlak & Ortiz, 1986): mode 1, early events without reopenings; mode 2a, short single late openings; and mode 2b, bursts of late openings. Since the whole-cell recordings of the mutant had shown increased I_{ss}/I_{peak} ratios, the late Na^+ currents were quantified for each pulse and normalized with respect to the average peak current (I_{late}/I_{peak}). In 'diary plots' (Fig. 4*C* and *D*), the higher peaks represent bursts of late openings (mode 2b), whereas the amplitude of a lower peak corresponds to the number of short single late openings (mode 2a). For all depolarization steps (100–300 per patch), the means of I_{late}/I_{peak} were significantly higher with V1589M (e.g. 1·14 ± 0·28% at −30 mV) than with the WT channel (0·31 ± 0·11% at −30 mV). The data obtained for a wide range of potentials are detailed in Fig. 4*E*. The occurence of late openings with the mutant was 3·7-fold more frequent (at −30 mV). When comparing this result with the whole-cell data, one has to take into account that the position of the inactivation curve of Na^+ channels measured in the cell-attached mode is shifted with respect to the whole-cell result (Fahlke & Rüdel, 1992). At −15 mV, the whole-cell measurements had shown that the I_{ss}/I_{peak} ratio is 3·7-fold larger for mutant than for WT channels, in perfect agreement with the single-channel result at −30 mV.

The rate of the late openings could be higher in mutant than in WT channels because either gating mode 2a or 2b occurs more frequently. To test this, we calculated the probability of WT and mutant channels entering these modes using the following equation: $a = nP(1-P)^{n-1}$, where P is the probability of the channel getting into either mode 2a or 2b, n is the number of channels present in the patch and a is the number of observed bursts or short late openings divided by the number of analysed traces. Since the bursting mode was infrequent, P was small and the equation was simplified to $P = a/n$. The probabilities for the mutant Na^+ channel to enter either mode 2a or 2b was significantly larger (2a: 0·40 ± 0·09; 2b: 0·011 ± 0·003, at −30 mV, $n = 6$ patches) than for the WT channel (2a: 0·06 ± 0·02; 2b: 0·003 ± 0·001, at −30 mV, $n = 6$).

Mean open times were analysed separately for gating modes 2a and 2b. Open time histograms were fitted with

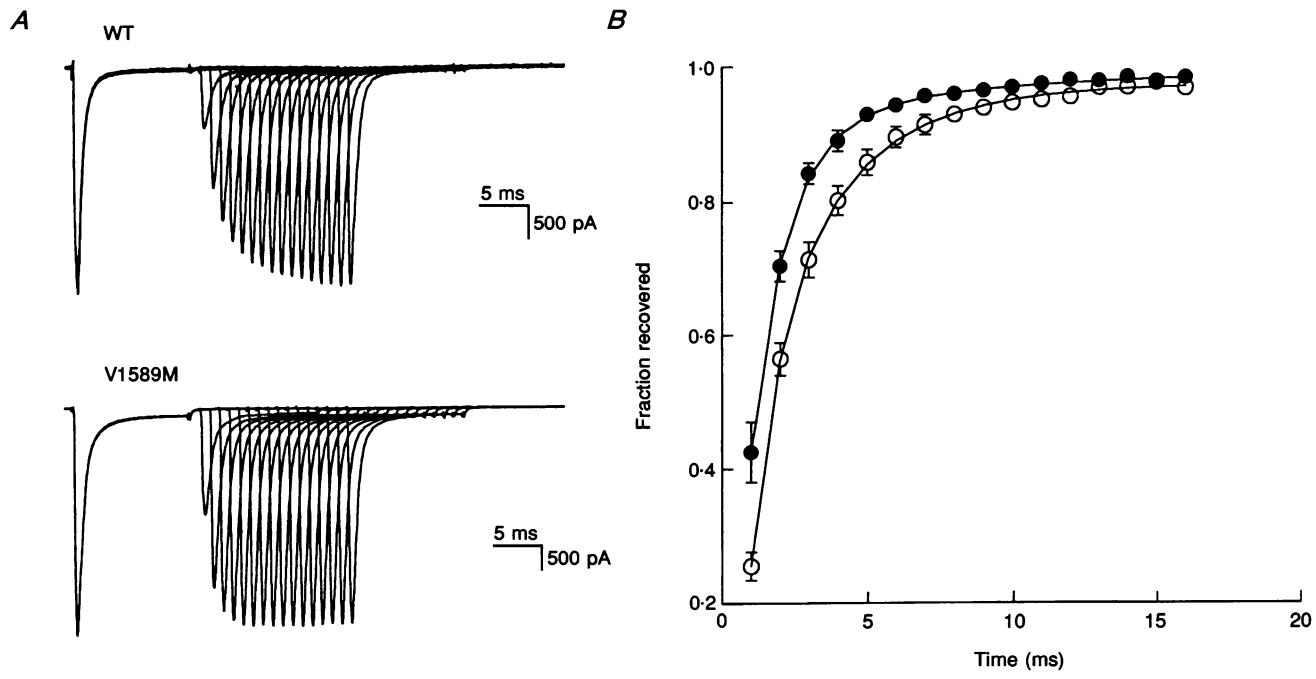

Figure 3. Recovery from inactivation
A, representative WT and V1589M current traces illustrating faster mutant recovery from inactivation. Cells held at −100 mV, depolarized for 12 ms to 0 mV and brought back to −100 mV for increasing durations before test pulse to 0 mV. *B*, Na^+ WT (○, $n = 9$) and V1589M (●, $n = 8$) channel recovery time. Plotted lines are double exponentials. The time constants for recovery from inactivation (τ_{r1} and τ_{r2}) were decreased from 1·28 ± 0·12 to 0·92 ± 0·08 ms and from 4·74 ± 0·94 to 2·66 ± 0·51 ms for the WT and mutant channels, respectively.

exponentials with average time constants of 0·18 ± 0·02 ms (mode 2a; $n = 5$), 1·42 ± 0·28 ms (mode 2b; $n = 3$) for WT channels and 0·20 ± 0·02 ms (mode 2a; $n = 5$), 1·31 ± 0·24 ms (mode 2b; $n = 4$) for mutant channels. For both modes the mean open times were similar in WT and mutant channels. Since not enough patches with only one channel were collected, records containing one to four channels were analysed.

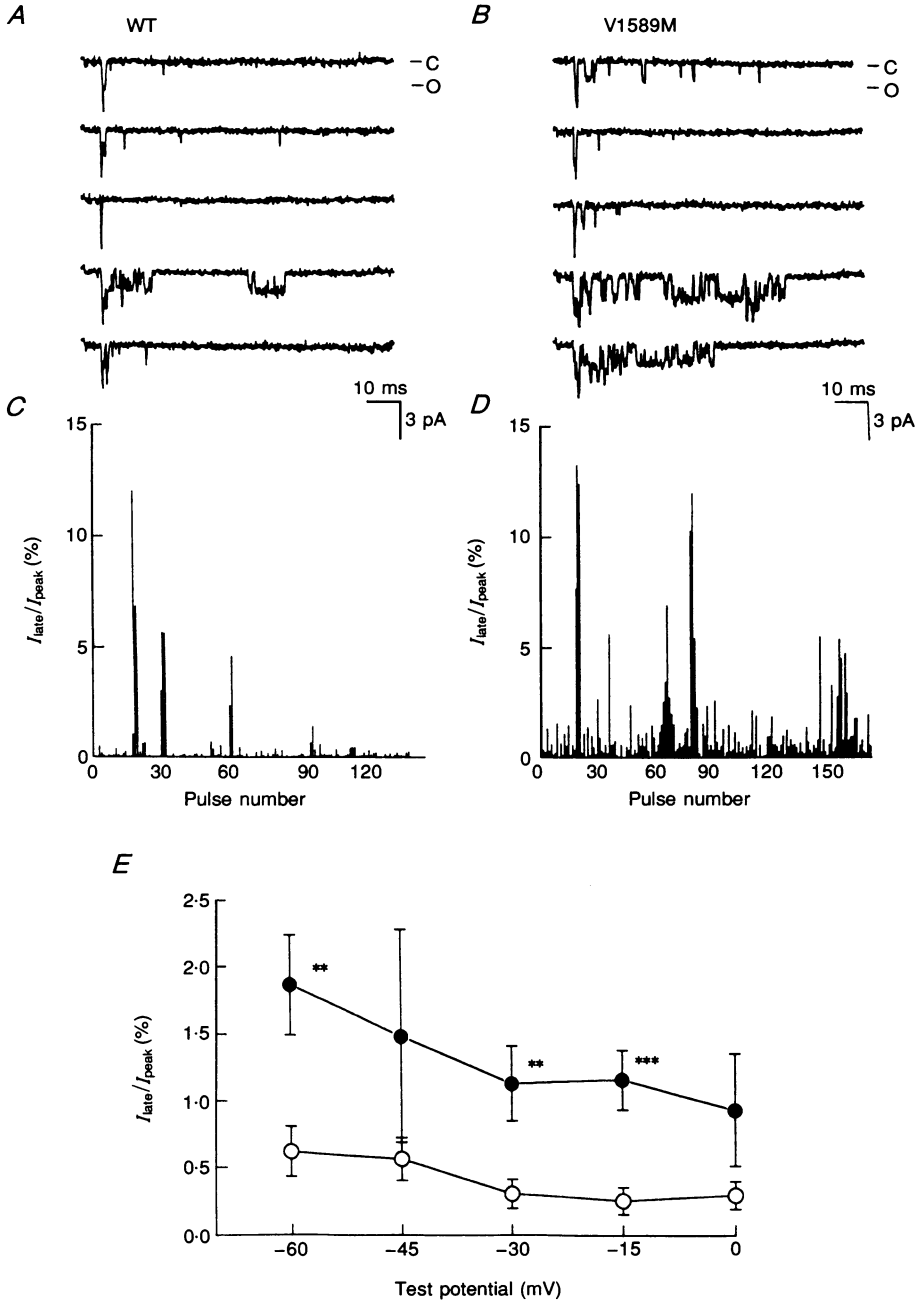

Figure 4. Late currents with WT and V1589M Na^+ channels

A, single-channel activity from a cell expressing WT channels. Currents elicited by steps going from −100 to −30 mV. Traces filtered with 2 kHz, (C, closed; O, open). *B*, single-channel activity from a cell expressing V1589M channels. Same recording protocol as in *A*. *C* and *D*, the current induced by late channel openings beginning 15 ms after the onset of the depolarization was calculated for each sweep by multiplication of the open probability with the single-channel amplitude. The relative current contribution of late openings were determined by use of this late current and the average early peak current (I_{late}/I_{peak}). *E*, evaluated WT (○, $n = 9$–12) and V1589M (●, $n = 6$–11) means of I_{late}/I_{peak} for several test potentials ± S.E.M. are shown. ***$P < 0{\cdot}001$, **$P < 0{\cdot}02$.

Cumulative latency distributions were also analysed and fitted with a single exponential. The time constants were larger ($\tau = 0{\cdot}59 \pm 0{\cdot}14$ ms) for mutant than for WT ($\tau = 0{\cdot}27 \pm 0{\cdot}06$ ms, both at -30 mV, $n = 6$) channels but this difference was not statistically significant ($P > 0{\cdot}05$, Student's t test).

The single-channel conductance was determined by evaluation of the late Na^+ channel openings and was 15 ± 1 pS ($n = 6$) for WT and 14 ± 1 pS ($n = 6$) for mutant channels.

How do the data from mutant channels fit with proposed models of the sodium channel?

Although the structure and function of the Na^+ channel is not completely understood, there is an agreement that it can assume either of three functional states: closed (C), activated or open (O) and inactivated (I). In the frame of the Horn & Vandenberg (1984) model, the faster recovery from inactivation obtained with the V1589M mutant indicates an increased transition rate from I to C, thus increasing the probability of the channel to reopen. On the other hand, an increased I_{ss}, as found with the V1589M mutant, could result from reopenings of the channels that occur following the transition I to O. Thus both a faster recovery from inactivation and a larger I_{ss} indicate a pronounced instability of the inactivated state.

Genotype–phenotype relationships

Studies on mutant Na^+ channels expressed in mammalian cells have revealed different mechanisms of Na^+ channel dysfunction. Chahine *et al.* (1994) examined the R1448H/C mutants causing paramyotonia congenita and proposed a model in which Na^+ channel inactivation is uncoupled from activation. They fitted the inactivation time course of the mutant channel with one time constant which showed no voltage dependence. They did not observe Na^+ channel modal gating either in mutant or in WT channels but, as they pointed out, the depolarizing pulses were probably too short to observe it. Our data do not fit their model since the inactivation time constants (τ_{h1} and τ_{h2}) were clearly voltage dependent. Furthermore, we observed modal gating in both WT and mutant channels.

Cummins *et al.* (1993) examined the HyperPP mutant T704M and reported a shift of the activation curve producing a larger 'window current', but no effect on steady-state inactivation and recovery. In contrast, Cannon & Strittmatter (1993) reported an increased steady-state current and a modal gating pattern for both HyperPP mutants (T704M and M1592V).

Since V1589M is close to the M1592V mutation in the sixth segment of the fourth domain, and both produce a similar defect in Na^+ channel inactivation, the question arises of how they produce completely different clinical symptoms. The difference between the two phenotypes, stiffness *versus* paralysis, could be due to a different degree of depolarization caused by an inactivation defect. Slight depolarization could cause hyperexcitability and stiffness ($I_{ss}/I_{peak} = 3$–4%, V1589M; our results), a larger depolarization inexcitability and paralysis ($I_{ss}/I_{peak} = 7{\cdot}5\%$, M1592V; Cannon & Strittmatter, 1993).

The functional consequences of the V1589M and M1592V mutations could be explained on the molecular level. Since they are both located close to the cytoplasmic surface and both disturb the inactivation process, we hypothesize that this region of the channel protein may serve as an acceptor for the inactivation gate.

REFERENCES

Aldrich, R. W., Corey, D. P. & Stevens, C. F. (1983). A reinterpretation of mammalian sodium channel gating based on single channel recording. *Nature* **306**, 436–441.

Cannon, S. C., Brown, R. H. & Corey, D. P. (1991). A sodium channel defect in hyperkalemic periodic paralysis: K^+ induced failure of inactivation. *Neuron* **6**, 619–626.

Cannon, S. C., Brown, R. H. & Corey, D. P. (1993). Theoretical reconstruction of myotonia and paralysis caused by incomplete inactivation of sodium channels. *Biophysical Journal* **65**, 270–288.

Cannon, S. C. & Corey, D. P. (1993). Loss of Na^+ channel inactivation by anemone toxin (ATX II) mimics the myotonic state in hyperkalaemic periodic paralysis. *Journal of Physiology* **466**, 501–520.

Cannon, S. C. & Strittmatter, S. M. (1993). Functional expression of sodium channel mutations identified in families with periodic paralysis. *Neuron* **10**, 317–326.

Chahine, M., George, A. L., Zhou, M., Ji, S., Sun, W., Barchi, R. L. & Horn, R. (1994). Sodium channel mutations in paramyotonia congenita uncouple inactivation from activation. *Neuron* **12**, 281–294.

Cummins, T. R., Zhou, J., Sigworth, F. J., Ukomadu, C., Stephan, M., Ptacek, L. J. & Agnew, W. S. (1993). Functional consequences of a Na^+ channel mutation causing hyperkalemic periodic paralysis. *Neuron* **10**, 667–678.

Fahlke, Ch. & Rüdel, R. (1992). Giga-seal formation alters properties of sodium channels of human myoballs. *Pflügers Archiv* **420**, 248–254.

George, A. L., Komisarof, J., Kallen, R. G. & Barchi, R. L. (1992). Primary structure of the adult human skeletal muscle voltage dependent sodium channel. *Annals of Neurology* **31**, 131–137.

Graham, F. L. & van der Eb, A. J. (1973). A new techique for the assay of infectivity of human adenovirus 5 DNA. *Virology* **52**, 456–467.

Hamill, O. P., Marty, A., Neher, E., Sakmann, B. & Sigworth, F. J. (1981). Improved patch-clamp techniques for high-resolution current recording from cells and cell-free membrane patches. *Pflügers Archiv* **391**, 85–100.

Heine, R., Pika, U. & Lehmann-Horn, F. (1993). A novel SCN4A mutation causing myotonia aggravated by cold and K^+. *Human Molecular Genetics* **9**, 1349–1353.

Horn, R. & Vandenberg, C. A. (1984). Statistical properties of single sodium channels. *Journal of General Physiology* **84**, 505–534.

Isom, L. L., De Jongh, K. S., Patton, D. E., Reber, B. F. X., Offord, J., Charboneau, H., Walsh, K., Goldin, A. L. & Catterall, W. A. (1991). Primary structure and functional expression of the β_1 subunit of the rat brain sodium channel. *Science* **256**, 839–842.

LEHMANN-HORN, F., IAIZZO, P. A., HATT, H. & FRANKE, C. (1991). Altered gating and conductance of Na^+ channels in hyperkalemic periodic paralysis. *Pflügers Archiv* **418**, 297–299.

LEHMANN-HORN, F., KÜTHER, G., RICKER, K., GRAFE, P., BALLANYI, K. & RÜDEL, R. (1987). Adynamia episodica hereditaria with myotonia: a noninactivating sodium current and the effect of extracellular pH. *Muscle and Nerve* **10**, 363–374.

LERCHE, H., HEINE, R., PIKA, U., GEORGE, A. L., MITROVIĆ, N., BROWATZKI, M., WEISS, T., RIVET-BASTIDE, M., FRANKE, C., LOMONACO, M., RICKER, K. & LEHMANN-HORN, F. (1993). Human sodium channel myotonia: slowed channel inactivation due to substitutions for a glycine within the III–IV linker. *Journal of Physiology* **470**, 13–22.

PATLAK, J. B. & ORTIZ, M. (1986). Two modes of gating during late Na^+ channel currents in frog sartorius muscle. *Journal of General Physiology* **87**, 305–326.

ROJAS, C. V., WANG, J., SCHWARTZ, L., HOFFMAN, E. P., POWELL, B. R. & BROWN, R. H. (1991). A Met-to-Val mutation in the skeletal muscle sodium channel α-subunit in hyperkalemic periodic paralysis. *Nature* **354**, 387–389.

RÜDEL, R., RICKER, K. & LEHMANN-HORN, F. (1993). Genotype–phenotype correlations in human skeletal muscle sodium channel disease. *Archives of Neurology* **50**, 1241–1248.

Acknowledgements

We thank Dr R. Rüdel for discussions. This work was supported by the Deutsche Forschungsgemeinschaft (Le481/3-2), NIH grant AR01862 and the Muscular Dystrophy Association of the USA (F.L.H.). A.L.G. is at Lucille P. Markey School and was supported in part by a grant from the Lucille P. Markey Charitable Trust.

Received 29 April 1994; accepted 10 June 1994.